

E4-2007-157

V. N. Kondratyev¹, I. M. Kadenko²

NUCLIDE CREATION AND ANNEALING REACTOR
WASTE IN NEUTRON FIELDS

¹E-mail: Vkondrat@theor.jinr.ru

²Nuclear Physics Department, Taras Shevchenko National University
of Kiev, UA-03022 Ukraine

Кондратьев В. Н., Каденко И. М.

E4-2007-157

Образование нуклидов и отжиг отходов реакторов в нейтронных полях

Химические элементы во Вселенной (их свойства и превращения) рассматриваются как топливо, питающее эволюцию звезд, галактик и т. д. Реакции термоядерного синтеза представляют источник энергии звезд и, в частности, Солнца, питающего жизнь на Земле. Это порождает вопрос о происхождении и условиях возникновения жизни. Мы обсуждаем некоторые специфические особенности цепочек ядерных реакций при гидростатическом горении нуклидов в звездах и попытки создания термоядерных реакторов на Земле. Новые и сверхновые звезды рассматриваются как перспективные кандидаты астрофизических областей для синтеза тяжелых атомных ядер и возобновления других ядерных компонентов. При таком взрывном нуклеосинтезе образуются актиниды, являющиеся основным топливом для ядерных реакторов деления. Мы кратко анализируем e -, s - и r -процессы, принимая во внимание ультрасильное намагничивание в звездах, и обсуждаем некоторые идеи для отжига радиоактивных токсичных отходов атомной энергетики.

Работа выполнена в Лаборатории теоретической физики им. Н. Н. Боголюбова ОИЯИ.

Сообщение Объединенного института ядерных исследований. Дубна, 2007

Kondratyev V. N., Kadenko I. M.

E4-2007-157

Nuclide Creation and Annealing Reactor Waste in Neutron Fields

We consider chemical elements in the Universe (their properties and transmutations) as a fuel powering an evolution of stars, galaxies, etc. The nuclear fusion reactions represent an energy source of stars and, in particular, the Sun fitting the life on the Earth. This brings a question on an origin and conditions for creation of life. We discuss some specific features of nuclear reaction chains at the hydrostatic burning of nuclides in stars and treaties for development of thermonuclear fusion reactors at the Earth based environment. The nova and supernova give promising astrophysical site candidates for synthesis of heavy atomic nuclei and renewing other nuclear components. Such an explosive nucleosynthesis yields the actinides containing basic fuel for nuclear fission reactors, among others. We briefly outline the e -, s -, and r -processes while accounting for ultra-strong stellar magnetization, and discuss some ideas for annealing the radioactive toxic nuclear waste.

The investigation has been performed at the Bogoliubov Laboratory of Theoretical Physics, JINR.

Communication of the Joint Institute for Nuclear Research. Dubna, 2007

1. THE NUCLEAR FUEL

It is commonly recognized by past that the energy driving an evolution of many sites of the Universe, e.g., biological species on the Earth, stars, galaxies, comes from nuclear reactions, i.e., the reactions involving atomic nuclei. Therefore, the studies of nuclear matter are crucial for learning and exploring such a renewable source of energy. The binding energy of nucleon aggregates, i.e. atomic nuclei, represents the first clue for an understanding of basic properties of the nuclear fuel. As is seen in Fig.1 the transition metals of iron series represent the most tightly bound nuclides marking a bottom of fusion–fission valleys on the nuclear binding energy chart discovered at the Earth based laboratory.

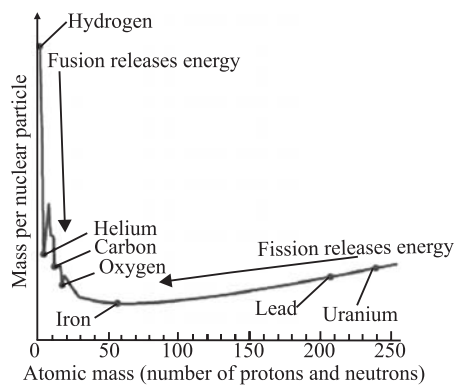


Fig. 1. Schematic view of stable nuclide binding energy versus mass number, cf. Ref. [1]

As a consequence the energy can be released either in the fusion reactions of nuclides which are lighter than iron or in the fission of heavy atomic nuclei with mass numbers larger than 56. This property gives basic concepts for nuclear fission and thermonuclear fusion reactors with fundamental consequences on origin and processing the nuclear fuel.

2. THE STARS IN THE HERTZSPRUNG–RUSSELL DIAGRAM

We now start a discussion of hydrostatic burning of atomic nuclei in stars, i.e., the main sequence stars giving a track in the Hertzsprung–Russell diagram, or HR diagram. The HR diagram represents a plot on a plane where the ordinate (vertical) axis is the luminosity while the absciss (horizontal) axis shows the surface temperature (as measured by a color of a star). Stellar luminosities vary from 10^{-4} to 10^6 that of our Sun, with surface temperatures ranging, respectively, from 2000 to 50000 K.

The most obvious specific characteristics of a star are respective surface temperature T_s , luminosity L , and radius R . The former two are accessible to observation, but the radius is generally not. Yet a relationship between these properties can be easily specified. Pretending the stars radiate as black bodies, the energy emission rate per unit surface area is given by the Stefan–Boltzmann black-body radiation law, σT_s^4 , with the constant $\sigma = 5.67 \cdot 10^{-5}$ ergs/K⁴/s/cm². Thus the star’s luminosity is given by $L = 4\pi R^2 \sigma T_s^4$. Normalizing observables to solar properties, this relation can be rewritten as

$$\frac{L}{L_{\text{solar}}} = \left(\frac{R}{R_{\text{solar}}} \right)^2 \left(\frac{T_s}{T_{\text{solar}}} \right)^4.$$

Though this result is true only for a black body, it makes it plausible that a plot of luminosity versus temperature might yield a one-dimensional path in the plane parameterized by the radius. For example, given class of stars radiates according to the Stefan–Boltzmann law, their characteristics (T_s, L, R) would follow the trajectory as described above.

This was basically the discovery of Hertzsprung and Russell. The HR diagram in Fig. 2 shows a dominant trajectory — the main sequence — running from high to low temperature. It also shows other classes of stars that reside well off the main sequence. The Sun is situated on the main sequence according to observed solar surface temperature of about 6500 K. Stars at the upper left, i.e., on the main sequence with temperatures of 4 times that of the Sun and luminosities of 6 orders of magnitude larger, would have a radius of about 60 times that of our Sun. The red, cool, dwarf stars at the lower right of the main sequence, with luminosities of about 2000 times lower than that of the Sun and temperature of

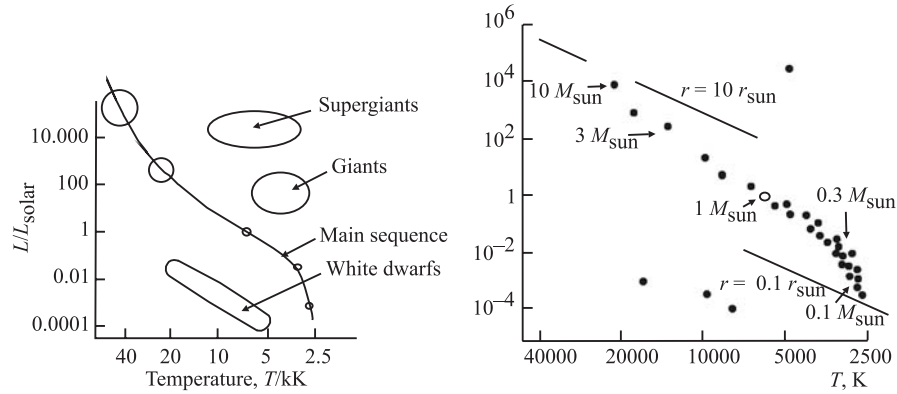


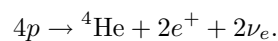
Fig. 2. Schematic illustration of main-sequence sections at the HR diagram, including the position of the Sun (right panel)

about a half of the solar one, have radii of about 0.1 that of the Sun. Other classes of stars are well separated from the main sequence. One group has luminosities of the order of 10^4 and temperatures again of about a half from that of the Sun. Thus, these supergiants would correspond to a radius of about 400 times that of the Sun. Red giants, which form another patch off the main sequence, have a radius of about 50 times than that of the Sun. White dwarfs — with luminosities of about 1/200 of solar and temperatures of twice solar — would correspond to a radius of about 1/50 that of the Sun. These objects sit well below the main sequence.

3. THE STANDARD SOLAR MODEL AND THE pp CHAIN

We consider now the stars burning hydrogen through the pp and the CNO cycles, such as the Sun and similar stars. Almost all stars lying along the main sequence (perhaps 80% of the stars observed) are thought to be hydrogen burning. Evidently, the Sun gives our «test case» for developing a theory of main-sequence stellar evolution. We know far more about this star, e.g., the age, luminosity, radius, surface composition, and even its neutrino luminosity and helioseismology, than of any other star. Solar models trace the evolution of the Sun over the past 4.6 billion years of main sequence burning, thereby predicting the present-day temperature and composition profiles of the solar core that govern energy production. Standard solar models share four basic assumptions:

- The Sun evolves in hydrostatic equilibrium, maintaining a local balance between the gravitational force and the pressure gradient. To describe this condition in detail, one must specify the equation of state at various compositions.
- Energy is transported by radiation and convection. While the solar envelope is convective, radiative transport dominates in the core region where thermonuclear reactions proceed. The opacity depends sensitively on the solar composition, particularly the abundances of heavy elements.
- Thermonuclear reaction chains generate solar energy. As is considered within the Standard Model, this energy is produced from the conversion of four protons into ${}^4\text{He}$, generally, written as



About 98% of this synthesis occurs through the pp chain, with the CNO cycle contributing the remaining 2%. The Sun is a large but slow reactor since the core temperature $T_c \sim 1.5 \cdot 10^7$ K results in typical center-of-mass

energies for reacting particles of ~ 10 keV, much less than the Coulomb barrier suppressing charged particle nuclear reaction. Thus reaction cross sections are small, and one should probe significantly higher energies before laboratory measurements are feasible. These laboratory data must then be extrapolated to the solar energies of interest.

- The model is constrained to produce today's solar radius, mass, and luminosity. An important assumption of the Standard Model is that the Sun was highly convective, and therefore uniform in composition, when it first entered the main sequence epoch. It is further presumed that the surface abundances of metals (nuclei with mass numbers $A > 5$) were undisturbed by the subsequent evolution providing, thereby, a record for the initial solar metallicity. The remaining parameter is the initial ${}^4\text{He}/\text{H}$ ratio, which is adjusted until the model reproduces the present solar luminosity after 4.6 By of evolution. The resulting ${}^4\text{He}/\text{H}$ mass fraction ratio is typically 0.27 ± 0.01 , which can be compared to the Big-Bang value of 0.23 ± 0.01 .

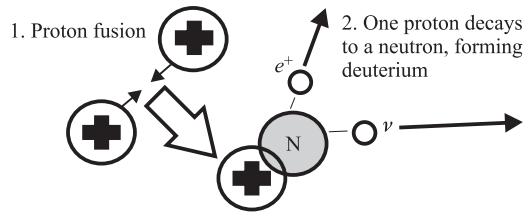
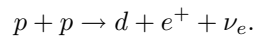


Fig. 3. Schematic view of pp fusion process

The emerging «standard solar model» describes the evolving Sun. Predominant component in the energy emerges from the pp chain. There is clearly no strong or radiative capture reaction that can initiate ${}^4\text{He}$ synthesis in the Sun. The $p + p$, $p + {}^4\text{He}$ and ${}^4\text{He} + {}^4\text{He}$ reactions do not release energy and thus do not form bound states. The driving reaction of the pp chain is governed by a weak interaction



This is analogous to neutron or nuclear decay, except that the initial state is not given as a nucleus, but as two protons in plasma. The cross section is very small, about 20 orders of magnitude below the strong interaction S -factors, and cannot be measured at the laboratory. Thus our description of the basic process that powers the majority of stars has to be taken from the first principles

of nuclear theory calculations. As is believed, this can be done to an accuracy of about 1% to give the astrophysical factor

$$S_{pp} = 0.41 \cdot 10^{-21} \text{ keV} \cdot \text{b}.$$

In the core of the Sun, at temperature $T_c \sim 15 \text{ MK}$ and proton density of $3 \cdot 10^{25}/\text{cm}^3$, the $p+p$ -reaction rate can be calculated to give $r_{pp} \sim 0.6 \cdot 10^8 / \text{cm}^3/\text{s}$. Therefore, the time scale for burning hydrogen is the number density divided by twice the burning rate (two protons are consumed per reaction) and calculated to be $t_{\text{sun}} \sim 7.9 \text{ By}$. It can be compared to the Sun's present age, 4.55 By, or about half its lifetime.

Once the initiating $p + p$ decay reaction occurs, we can see relatively easy how the rest of the burning might proceed, e.g.,

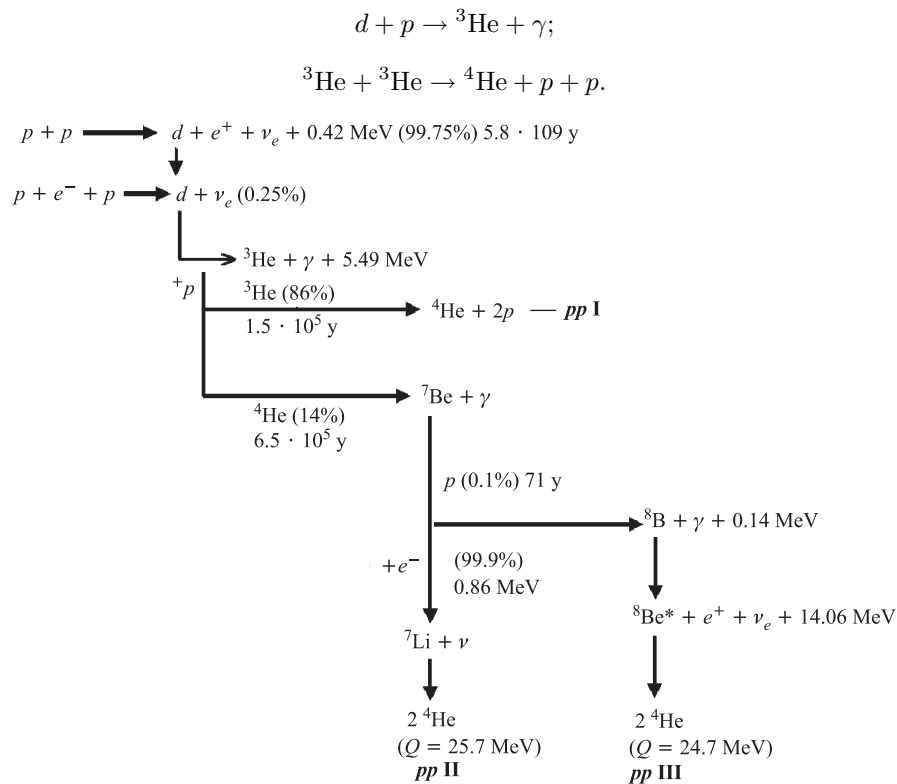


Fig. 4. The competition between the pp reaction chains

This is the so-called *pp* I cycle making, indeed, the most robust part of the *pp* chain in stars with nearly solar temperatures. About 90% of ${}^4\text{He}$ produced today in the solar core is predicted to be synthesized in this way. Somewhat less important branches for the *pp* chain are shown in Fig. 4.

3.1. Nuclear Fusion Reactors. For potential nuclear energy sources at the Earth based environment, the deuterium–tritium fusion reaction contained by some kind of the magnetic confinement, e.g. the Tokamak, shown schematically

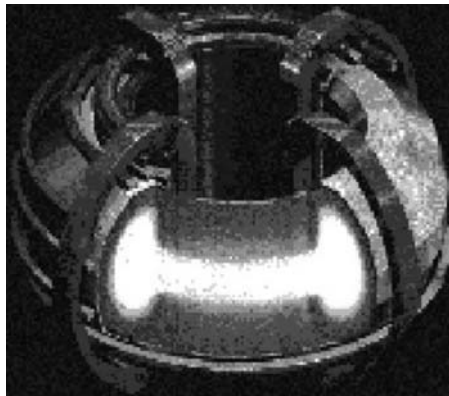


Fig. 5. Schematic view of the Tokamak

in Fig. 5, seems the most likely path. At the fusion of deuterium and tritium the reaction yields about 17.6 MeV of energy release but requires a high temperature (of about million Kelvins) to overcome the Coulomb barrier and ignite the fuel. The deuterium fuel component is naturally abundant, but tritium must be either bred from lithium or got in the operation of the deuterium cycle. It is worthy to recall in this regards the famous International Thermonuclear Experimental Reactor (ITER) project aiming to demonstrate the scientific and technical feasibility of fusion power.

3.2. Hydrostatic Burning in Massive Stars. We come to a massive star, in excess of 10 solar masses, burning the hydrogen in its core under the conditions of hydrostatic equilibrium. When the hydrogen is exhausted, the core contracts until the density and temperature rise to stimulate noticeable $3\alpha \rightarrow {}^{12}\text{C}$ process. The ${}^4\text{He}$ comes then over, etc. The pattern, i.e., fuel burned to exhaustion, contraction, and ignition of the ashes from the previous burning cycle, repeats several times (cf. Fig. 6), leading finally to the explosive burning of ${}^{28}\text{Si}$ to Fe. For a heavy star, the evolution is rapid: the star has to work harder to maintain the hotter electron gas necessary to sustain itself against its own gravity, and therefore consumes its fuel faster. Likewise, as the star contracts to higher density after each burning stage, and because the energy liberated in late-stage burning cycles is modest (cf. Fig. 1), the evolution accelerates as the star progresses to later stages. A 25 solar mass star would go through all of these cycles in about 7 My, with the final explosion Si burning stages taking a few days. The resulting «onion skin» structure of the precollapse star is shown in Fig. 6. Note that one can read through the nuclear history of the star by going from the surface and outer skin inward.

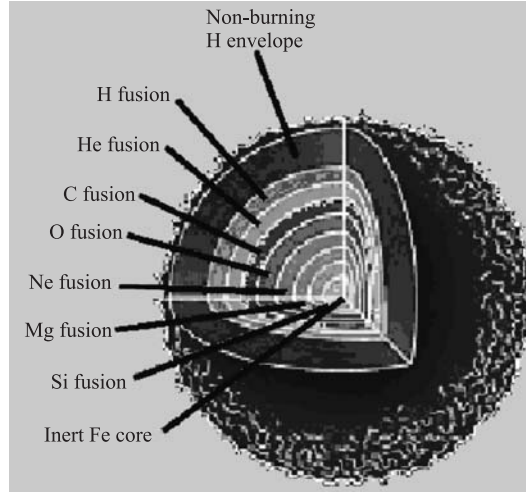
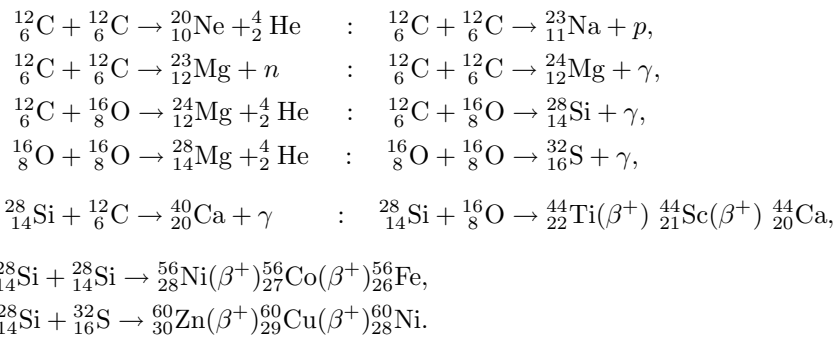


Fig. 6. The view of «onion structure» of massive stars

The reaction sequences are the following (cf. Fig. 6):

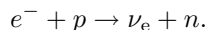


Once the Si burns to produce Fe, there is no further source of nuclear energy adequate to support the star. So as the last remnants of nuclear burning take place, the core is largely supported by degeneracy pressure, with the energy generation rate in the core being less than the stellar luminosity. The core density is of about $2 \cdot 10^9$ g/cc and the temperature is $kT \sim 0.5$ MeV.

4. CORE-COLLAPSE SUPERNOVAE

As is pointed out in Subsec. 3.2, the gravitational collapse that begins with the end of Si burning is not halted by a new burning stage, but continues. As gravity

does work on the matter, the collapse leads to a rapid heating and compression of the matter. As the nucleons in Fe are bound by about 8 MeV, sufficient heating can release γ s and few nucleons. At the same time, the electron chemical potential is increasing. This makes favorable the electron capture on nuclei and any free protons, i.e.,



While the chemical equilibrium is reached, an equality for chemical potentials reads

$$\mu_e + \mu_p = \mu_n + \langle E_\nu \rangle.$$

Therefore, the fact that neutrinos are not trapped plus the rise in the electron Fermi surface as the density increases, leads to increased neutronization of the matter. The escaping neutrinos carry off energy and lepton number. Both the electron capture and the nuclear excitation and dissociation take energy out of the electron gas, which is the star's only source of support. This means that the collapse is very rapid. Numerical simulations find that the iron core ($\sim 1.2 - 1.5$ solar masses) of the star collapses at about 0.6 of the free fall velocity.

In the early stages of the infall the ν_e s readily escape. But neutrinos are trapped at a density of $\sim 10^{12}$ g/cm³. At this point the neutrinos begin to scatter of the matter through both charged current and coherent neutral current processes coming to a «random walk» out of the star core. When the neutrino mean-free-path becomes sufficiently short, the «trapping time» of a neutrino begins to exceed the time scale for the collapse to be completed. This occurs at a density of about $\sim 10^{12}$ g/cm³, or somewhat less than 1% of nuclear saturation density. After this point, the energy released by further gravitational collapse and the star's remaining lepton number are trapped within a proto-neutron star. If we take the respective neutron star mass M of 1.4 solar masses and a radius R of 10 km, a rough estimate of its binding energy gives the value $\frac{GM^2}{2R} \sim 2.5 \cdot 10^{53}$ ergs. This is roughly the trapped energy that will be later on radiated in neutrinos.

The collapse of the homologous core continues until densities reach nuclear saturation values. Nuclear matter is rather incompressible ($K \sim 200$ MeV/fm³). While the innermost shell of a star is compressed to densities of 3–4 times of normal nuclear density (e.g., perhaps $6 \cdot 10^{14}$ g/cm³), it first rebounds sending a pressure wave out through the homologous core. This wave travels faster than the infalling matter, since the homologous core is characterized by a sound speed in excess of the infall speed. Subsequent shells follow to be heated up. The resulting series of pressure waves collects near the sonic point (the edge of the homologous core). As at this point density attains the nuclear saturation numbers and comes to rest, a shock wave breaks out and begins its traversal of the outer

core. Thus, the shock wave is formed at the boundary of the homologous core, i.e., at the point where supersonic becomes subsonic.

The shock wave melts the iron core and stalls in the outer iron core, before it reaches the point just outside the iron core where the shock can (in principle) deliver enough energy to the matter to lift it off the star. Note that the supernova problem is entirely one of energy transfer: all matter in the star was initially bound. Thus the energy released by the core in falling deep into a gravitational potential must be transferred to the mantle to create an explosion. As a matter of fact, mechanism of sufficiently efficient energy transfer remains an open problem. Dissipation due to shock wave heating of matter and neutrino emission reduces to negligible numbers of energy transfer efficiency by the shock wave. So that the mechanism of SN explosion is not understood.

4.1. Convection and Magnetization. A current large-scale computing grand challenge is 2D modeling [2] to explore a possibility that convection might help to achieve explosions. Substantial evidences from SN1987A and other supernovae (e.g., explosion asymmetry, early emission of X-rays and γ rays, and outward mixing of ^{56}Ni) point to an occurrence of convective dynamics during supernova events. This specific feature is strongly corroborated by numerical simulations [2] indicating the development of strong convection when high-entropy material, heated up from central core by neutrinos, rises and is replaced by cool matter from upper layers. Such a violent convection results in magneto-rotational instabilities and/or dynamo-action bringing enormous amplification of stellar magnetization. Magnetic fields of strengths ranging up to hundred of *tera-tesla* represent plausibly an inherent feature of this spectacular astronomical phenomenon. Such a *magnetar* concept is strongly corroborated by numerous observations of soft gamma repeaters (SGRs) and anomalous X-ray pulsars (AXPs). These fields can, in fact, modify the structure of atomic nuclei [3] and give urgency to analyze possible magnetic effects in nuclide transformations. Incorporating such field effects in an analysis of nuclear reaction network may provide more insights on neutron stars and supernovae, e.g., magnetodynamics at neutron star crusts formation.

5. EXPLOSIVE NUCLEOSYNTHESIS

The explosion of a core-collapse supernova leads, nevertheless, to ejection of the star's mantle, and thus to substantial enrichment of the interstellar medium with the major burning products of hydrostatic equilibrium: ^4He , ^{12}C , ^{16}O , ^{20}Ne , etc., some among the most plentiful elements in nature. In this section we describe several nucleosynthesis mechanisms associated with the explosive conditions of a supernova (i.e., the *e*-, *s*-, and *r*-processes) while paying particular attention to magnetic effects.

Explosive nucleosynthesis denotes, therefore, the creation of elements by the explosion itself. The properties of this process are tied to those of the supernova event, which are still poorly understood, cf. Sec. 4. But the observation that the kinetic energy of a supernova explosion is typically in the range of $(1 - 4) \cdot 10^{51}$ ergs, provides an important constraint.

5.1. Nuclear Composition of Ultramagnetized Stellar Media. The nuclear statistical equilibrium (NSE) approximation in the theory of synthesis of chemical elements is used very successfully for the description of abundance of atomic nuclei with the greatest binding energy (i.e., transition metals of iron group and nearby nuclides) for over half a century. The magnetic field leads to an increase of nuclear reaction (transformation) rates [4] and, accordingly, to an acceleration of an establishment of statistical equilibrium. Therefore, we employ such an approach to consider an influence of magnetic fields on nuclide formation processes in stars. The detailed description of NSE model is widely presented in the literature, cf. [5]. Therefore, we recall here just basic steps, amendments, modifications and additions to NSE due to presence of a magnetic field.

Statistical equilibrium represents a condition of entropy S extreme $TdS = \sum_i \mu_i dY_i = 0$, indicating, thereby, that an abundance of the i th nuclear particle Y_i at a temperature T is determined by the respective nucleon chemical potential μ_i .

The thermodynamic formalism based on implications of self-consistent mean field approach for an analysis of baryon magnetism has been already described [3–5]. We just remind that at magnetic field strengths ($H \leq 10^{14}$ T) and temperatures ($T \sim 10^{9.5}$ K) the portion of chemical elements Y is mainly determined by binding energy B of corresponding atomic nuclei through the Saha equation $Y \propto \exp\{-B/T\}$.

The magnetization of stellar media brings, however, a sensitivity of nuclide creation processes to a projection of respective magnetic moment on the field direction. When accounting for thermal fluctuations of the spin projection on the field vector the dependence of relative output for nucleosynthesis products ($y = Y(H)/Y(0)$) on magnetic field strength H is defined by a change of binding energy $\Delta B = B(H) - B(0)$ in the field and by magnetic components in the partition function G . With exponential accuracy this ratio can be written as

$$y \simeq G_n^{-N} G_p^{-Z} G_i \exp\{\Delta B/kT\}. \quad (\text{SE})$$

Here the spin-magnetic part in the partition function is represented by $G_i = \sum_M \exp\{g_i M \omega_L / kT\} / (2I_i + 1)$ and is determined by an energy for an interaction of magnetic field with the magnetic moments of atomic nuclei $i = \frac{A}{N} Z$ with spin I_i , free N neutrons and Z protons, $g_{n(p,i)}$ gives g -factor of a neutron (proton, atomic nucleus), and $\omega_L = \mu_N H$ with a nucleon magneton μ_N . Two possible spin projections on a quantization axis for nucleons lead to relatively simple

form $G_N = \cosh[g_N\omega_L/2kT]$, while nucleon aggregates require explicit calculations.

5.1.1. Structure of Magnetized Atomic Nuclei. As is shown [3], shell effects dominate for atomic nuclei at considered magnetic field strengths. We recall here, that within the Hartree self-consistent mean field approach the single-particle energy levels determine the shell corrections. Applications of the Nilsson model are very successful in understanding of many properties of stable nuclei in the region of average mass numbers $A \sim 10 - 100$. Employing such a model one incorporates the harmonic oscillator (HO) spectrum of a frequency $\omega_0 \approx 41/A^{1/3}$ MeV and accounts for the spin-orbit splitting of energy levels with a gap $\eta_{so} \approx 0.12$ (in units ω_0).

Spin magnetization of Pauli type dominates for the neutron magnetic reactivity. Interaction of a field and the spin-magnetic moment corresponding to a spin projection m_n on a field vector gives rise to linear shift of energy levels $\Delta = m_n g_n \omega_L$. It results in a phase shift for a dependence of shell energy on neutron number. Magnetic response of protons is represented by a superposition of field interaction with spin and orbital magnetic moments. The presence of spin-orbit interaction results in abnormal dependence of proton shell correction energy on field strength. For instance, when the value of parameter $h = \omega_L/\omega_0$ approaches the strength of spin-orbit interaction η_{so} the shell oscillation amplitude can increase up to a factor of 5. Apparently, as seen in Fig. 7, total shell effect due to neutron and proton contributions at field strength $h = 0.07$ results in the most tightly bound nucleus of ^{44}Ti as compared to other symmetric nuclei.

5.1.2. Synthesis of Ultramagnetized Atomic Nuclei. As discussed above, an influence of a magnetic field is determined by shell structure of atomic nuclei. Thus, identifying magnetic field dependence of binding energy $\Delta B(H)$ with a change of shell correction energy C (i.e., $\Delta B \simeq C(H) - C(0)$) and using Eq. (SE), we examine some features of nuclide composition in ultra-magnetized astrophysical plasmas. The observations suggest that for nucleosynthesis NSE meet conditions of β -equilibrium with an equal amount of protons and neutrons (i.e. $Y_e = 0.5$). Consequently, production of symmetric ($N = Z$) nuclei prevails. Therefore, we consider relative outputs of nucleosynthesis products on an example of ^{56}Ni and ^{44}Ti often used for testing the supernova models. Apart from practical importance such a choice of symmetric atomic nuclei, double magic and antimagic at the Earth based laboratory, gives a transparent picture for an influence of magnetism on processes of formation of chemical elements with fundamental consequences on the nature of transmutation and synthesis of nuclides in superstrong magnetic fields.

As is evident from Fig. 8, oscillations of nuclide yields as a function of field strength represent perhaps the most interesting magnetic phenomenon. Change in the nuclear level structure caused by magnetic field results in rather different field dependence of relative abundance for ^{56}Ni and ^{44}Ti . Considering an increasing

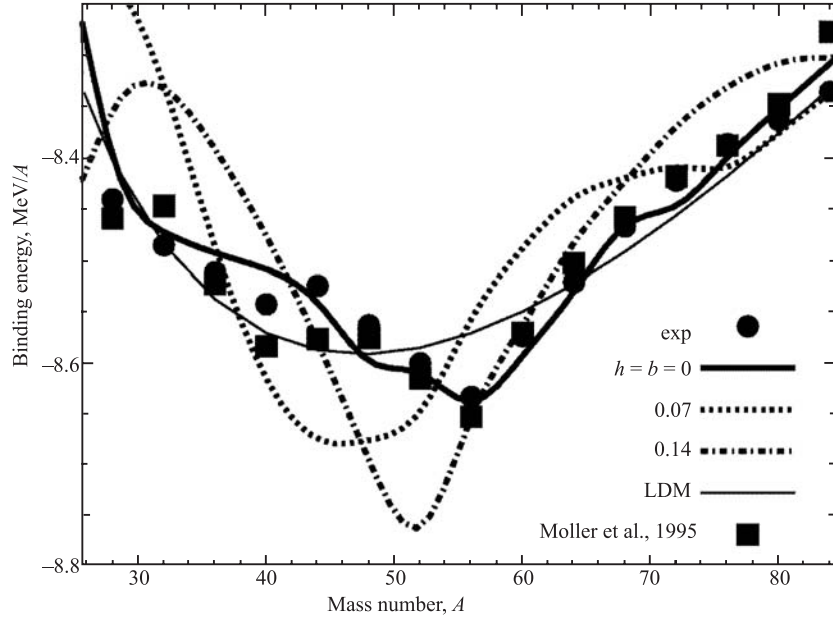


Fig. 7. Binding energy of even–even symmetric ($N = Z = A/2$) nuclei in the iron region. Thin and thick solid lines represent results of liquid drop model (LDM) without and with accounting for shell corrections [1]. Circles and squares illustrate experimental data and calculations by P. Moller et al. [6]. Dotted and dash-dotted lines show the results when taking into account modification of shell corrections due to magnetic fields $h = 0.07$ and 0.14 , accordingly

strength H in the range of relatively «weak» fields the production of ^{56}Ni is significantly suppressed, while the total volume of ^{44}Ti grows. Such a behavior is connected with magic–antimagic switching in nuclear shell structure in a variable magnetic field. For example, the slightly antimagic in laboratory nucleus of ^{44}Ti corresponds to growing binding energy at increasing field strength and becomes a magic nucleus at $h = 0.07$, cf. Fig. 7. At the same time, for nucleus of ^{56}Ni , double magic at the Earth conditions, the contribution of shell energy at such «weak» fields decreases. As a result, an output of ^{44}Ti considerably exceeds the yield of ^{56}Ni .

5.2. Abundances above the Iron Peak and Neutron Capture. Figure 9 shows the abundance pattern found in our solar system. We discussed above the origin of abundant light nuclei, especially the H, ^4He , and small mass elements. The iron region is favored due to its strong binding, see Subsec. 5.1. Apart from the abundance peak near the iron group elements the lower abundances for heavier isotopes also display an interesting features, e.g., mass peaks around $A \sim 130$ and ~ 190 . Such a clear structure in the pattern of heavy elements is associated with

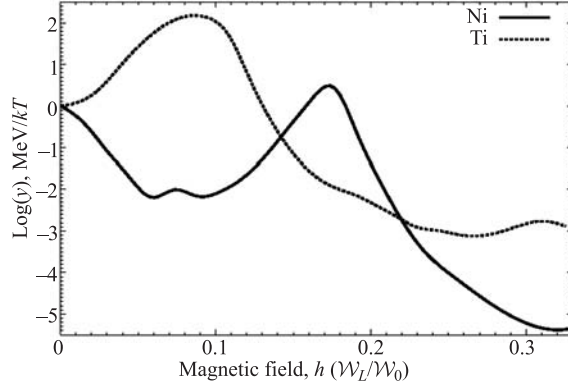


Fig. 8. Dependence on a magnetic field of relative yield $y_i = (Y_i(H)/Y_i)$ for ^{56}Ni (solid line) and for ^{44}Ti (dashed line) of nucleosynthesis at NSE conditions

the closed neutron shells in nuclear physics, i.e., the most stable configurations corresponding to the magic numbers $N = 50, 82,$ and 126 . Splitting of the abundance peaks suggests a presence of at least two contributing processes. The integrated abundance above the iron peak is not large, comparable to about 3% of the iron peak. Thus the responsible processes are reasonably rare.

This synthesis is associated with the neutron-capture reaction (n, γ) . The neutron sources emerge in stellar interiors, while neutron capture cross sections on heavy nuclei can be relatively large. As we see in the following sections, the observed shell structure naturally arises for such a process. Unstable but long-lived neutron-capture products, such as technetium, are observed in the atmospheres of red giants, indicating, thereby, an occurrence of neutron-induced synthesis in the cores of existing stars (and then dredged up to the surface).

Mechanisms for synthesizing heavy nuclei by capturing neutrons one at a time are represented by the s - and r -processes.

5.3. The s -Process. For the s -process the neutron capture proceeds in plasma containing neutrons and heavy seed nuclei at condition when the neutron capture rate is much slower than the typical β -decay rate. It brings then several consequences: 1) The weak interactions are then fast and maintain the $Z - N$ equilibrium: Every time when a neutron is captured, the resulting system of $A + 1$ nucleons has an opportunity for beta-decay to a nucleus of greater stability if such a nucleus exists, cf. Fig. 10. 2) The rate of synthesis is then proportional to the rate of neutron capture. The (n, γ) reactions control the «mass flow» to heavier nuclei. 3) The path of nucleosynthesis, due to point (1) above, proceeds along the so-called «valley-of-stability» on nuclear binding energy chart. These are the familiar nuclei studied at the Earth based laboratories.

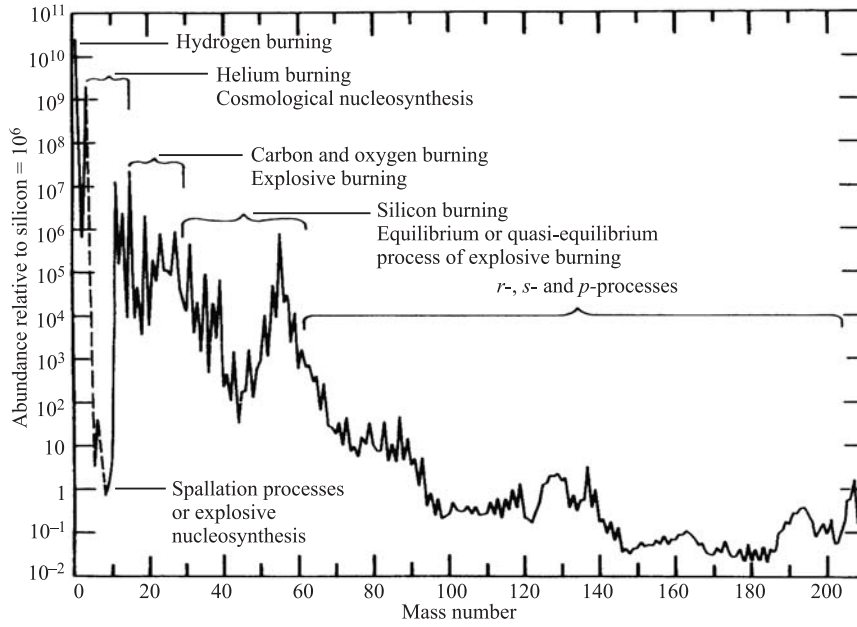


Fig. 9. Solar abundance

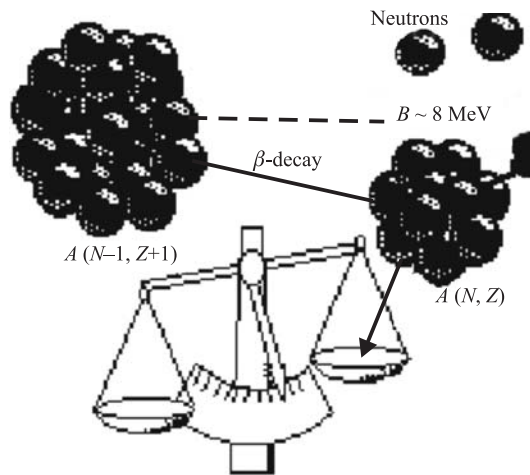


Fig. 10. Schematic view of the *s*-process sequence

It is easy to quantify the «slowness» of the s -process. The β -decay rates along the valley of stability are in the range from seconds to years. If one takes an average (n, γ) cross section of 0.1 b at 30 keV (corresponding to a neutron velocity of 0.008 c), the reaction rate per particle pair is evaluated to give $\langle\sigma v\rangle \approx 2.4 \cdot 10^{-17}$ cm³/s, and the capture rate per heavy nucleus is obtained by multiplying this by the neutron number density N_n . Thus, if we require $\tau_{(n,\gamma)} \geq 10$ y $\Rightarrow N_n \leq 10^8$ neutrons/cm³. While maintained for 2000 years, such a neutron density could synthesize $A \sim 200$ nuclei from iron group seeds.

One can also offer arguments to place a lower bound on the required neutron density. No stable nucleus exists at $N = 61$: there is, however, a long-lived isotope ^{107}Pd with half-life $\sim 7 \cdot 10^6$ y. Thus, if the neutron capture rate is too slow, ^{107}Pd will decay to ^{107}Ag , and neutron capture will then produce the stable nucleus ^{108}Ag . The nucleus ^{108}Pd will be bypassed. We conclude that neutron capture must be fast enough to synthesize ^{107}Pd in the s -process, and get the low limit $N_n > 10^2$ neutrons/cm³. This neutron number density then permits ^{108}Pd to be produced by guaranteeing that neutron capture is faster than the beta-decay in this case.

To quantify an abundance N_A of s -process nuclides we take the predominance of β decay if the channel is open and a constant neutron exposure $N_n(t) = N_n$. Then defining an average cross section $\langle\sigma v\rangle \cong \sigma_A \langle v\rangle$ over the Maxwell–Boltzmann distribution of relative velocities, the equation describing the mass flow in the s -process reads

$$\frac{dN_A}{dt} = \langle v\rangle N_n [\langle\sigma\rangle_{A-1} N_{A-1} - \langle\sigma\rangle_A N_A].$$

For equilibrium flow the LHS is zero and $\langle\sigma\rangle_{A-1} N_{A-1} = \langle\sigma\rangle_A N_A = \text{const}$. That is, the abundance achieved is inversely proportional to the neutron cross section. Evidently, the mass piles up at a target number with slow n -capture rate. Of course, the same argument goes through when the beta-decay is the destruction channel (and the beta-decay rate is presumably fast). The low-neutron capture cross sections at the closed shells should result in mass peaks, just as observation shown in Fig.9. It also follows that equilibrium will set in most quickly in the broad plateaus between the mass peaks since mass must pile up at the closed shells before the shell closure is breached. Thus, if the neutron flux is prematurely ended, the synthesis may not yet have gone beyond, for example, the $N \sim 82$ peak.

Several sites have been suggested for the s -process, but one well-accepted site is in the helium-burning shell of a red giant, where temperatures are sufficiently high to liberate neutrons by the reaction $^{22}\text{Ne}(^4\text{He}, n)^{25}\text{Mg}$, where ^{22}Ne is produced from alpha-capture sequence on the elements which the CNO cycle left after hydrogen burning.

Evidently, the s -process cannot proceed beyond ^{209}Bi while the neutron capture on this isotope leads to a decay chain that ends up with alpha-emission. This is a gap which the s -process cannot cross over. It follows that the actinides (e.g. transuranic elements) must have some other origin.

5.4. The r -Process. The s -process goes along the stability valley on the nuclear binding energy map while it is governed by β -stability. This path implies that in the valley some certain nuclei with an excess of neutrons will be missed in the s -process. Such nuclei can only be reached from the neutron-rich side requiring, thereby, another mechanism for synthesizing heavy nuclei. Such a second path proceeds through neutron-rich nuclei far from β -equilibrium conditions. Somewhat more convincing evidence is shown in Fig. 9, where the mass peaks at $A \sim 130$ and $A \sim 190$ are shown to split into two components, one corresponding to the expected s -process closed-neutron-shell peaks at $N \sim 82$ and $N \sim 126$, and the second one shifted to lower numbers $N \sim 76$ and ~ 116 .

This second process named the r - (or rapid-) process is characterized by the next properties. 1) The neutron capture is fast as compared to β -decay rates. Thus, 2) the equilibrium is maintained for $(n, \gamma) \longleftrightarrow \gamma, n$ component, cf. Fig. 11, i.e., neutron capture fills up the available bound levels in the nucleus until this equilibrium sets in. The new Fermi level depends on the temperature and the relative n/γ abundance. 3) The nucleosynthesis rate is thus controlled by the β -decay rate, each β^+ -transition converting $n \rightarrow p$ opens up a hole in the neutron Fermi sea allowing another neutron to be captured. 4) The nucleosynthesis path goes along exotic, neutron-rich nuclei that would be highly unstable under normal Earth based laboratory conditions.

In analogy with the s -process calculation of the previous Subsec. 5.3 for constant neutron exposure and equilibrated mass flow the system maintain $(n, \gamma \longleftrightarrow \gamma, n)$ equilibrium. This condition requires a balance between the rates for (n, γ) and (γ, n) reactions for an average nucleus, i.e.,

$$A + n \longleftrightarrow (A + 1) + \gamma.$$

Making use of the Saha equality (cf. Ref. [5]) one easily obtains the relationship between temperature T and neutron separation energy B along the r -process path at the density $N_n \propto kT^{3/2} \exp(-B/kT)$, cf. Fig. 11.

Using the conditions $N_n \sim 3 \cdot 10^{23}/\text{cc}$ and $T \sim 10^9$ K, we find the binding energy $B \sim 2.4$ MeV. Thus neutrons are bound by about 30 times of kT , still small value as compared to a typical binding energy of 8 MeV for a normal nucleus. As is mentioned above, the gaps exist at the magic numbers $N \sim 82$ and 126. When a shell closures gap is reached in the r -process, the neutron number of the nucleus remains frozed until the nucleus can change sufficiently to overcome the gap, i.e., to bring another bound neutron quantum level below the continuum. Thus N remains fixed while successive beta-decays occur. In

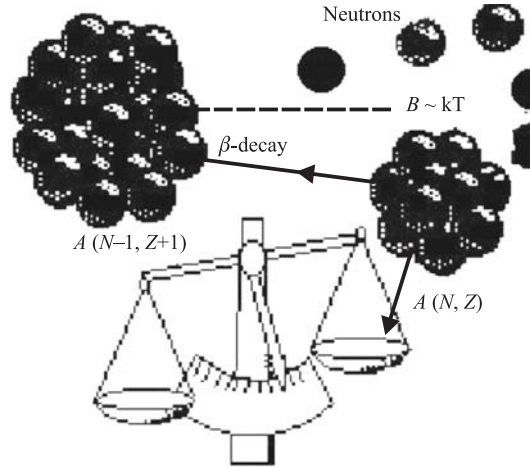


Fig. 11. Schematic view of the r -process sequence

the (N, Z) trajectory, the path goes along increasing Z with fixed N . Every beta-decay is followed by an (n, γ) reaction to fill the open neutron hole, but no further neutrons can be captured until the gap is overcome.

The closed neutron shells are called the «waiting points», because it takes a long time for the successive beta-decays to occur and to allow progression through nuclei with larger number N . The β decays are slow at the shell closures. Just as in the s -process, the abundance of a given isotope is inversely proportional to the β -decay lifetime. As a consequence the mass builds up at the waiting points, forming the spread abundance peaks seen in Fig. 9.

With removed neutron exposure the r -process comes to end by the beta-decay bringing nuclei back to the valley of stability. This can involve some neutron spallation (beta-delayed neutrons) that shifts the mass number A to a lower value. But it certainly involves conversion of neutrons into protons, and this shifts the r -process peaks at $N \sim 82$ and 126 to a lower N . This effect is clearly seen in the abundance distribution (see Fig. 9). Therefore, the s - and r -process peaks are splitted while the broader r -peaks are shifted towards small N relative to the s -process peaks.

The sites for the r -process have been debated many years and still remain a controversial subject. It is believed that the r -process can proceed to very heavy nuclei ($A \sim 270$) and finally comes to end by β -delayed and n -induced fission, which feeds matter back into the process at an $A \sim A_{\max}/2$. Thus there may be important cycling effects in the upper half of the r -process distribution. As is discussed in the next section such a fissile chain brings an option for incineration of radiotoxic waste of nuclear powerplants.

5.5. Annealing the Nuclear Reactor Waste. Thus, as is discussed in the previous section, the r -process explosive nucleosynthesis gives, in particular,

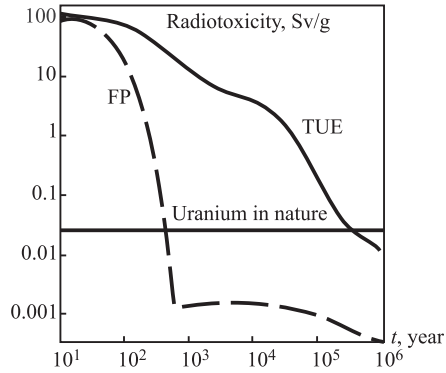


Fig. 12. Time dependence of the radiotoxicity for fission products (FPs) and transuranium elements (TUEs)

the actinides containing basic fuel for nuclear fission reactors, among others. Today processing and utilization of the burned nuclear fuel mark one of the most pronounced problems with the use of nuclear power. Light water reactor waste is mainly given by the burned reactor fuel containing two major element fractions, the actinides and the fission products (FPs). The actinides include the most radiotoxic components, especially, the transuranium elements (TUEs) like plutonium and the minor actinides (MA), neptunium, americium and curium. As is indicated in Fig. 12, the radiotoxicity of TUEs remains considerable for a

long time, up to Myears. At the same time, FPs have very short half-lives and can be disposed to the geological repository at upper level.

As we see in the proceeding sections the neutron exposure leads to very effective transmutation of atomic nuclei. This brings an idea to operate safely the fission reactor ashes commonly called the reactor waste. The neutrons might allow for incineration and transmutation the high level radioactive materials from nuclear powerplants in order to reduce the amount of the radiotoxicity and the half-life of radionuclides prior disposing in a geological repository. The incineration by neutron irradiation in a critical or subcritical assembly yields perhaps the most promising technique. The basic principle of those concepts is to induce nuclear reactions bringing the actinides to fission while the respective fission products are farther transmuted by neutron capture to short-lived and stable species (cf. Sec. 5). The controlled neutron source represents the main component of such an instrument.

We have already mentioned the thermonuclear fusion reactor producing an intense energetic (14 MeV) neutron field that might be used at the first wall of a magnetic confined fusion plasma for annealing nuclear waste. However, it is unlikely to be realized within a foreseeable future.

The accelerator-driven systems (ADS) provide an opportunity for relatively well-controlled neutron exposure and, therefore, represent promising setup for an analysis of experimental facility of this kind.

CONCLUSION

We briefly outlined here some basic properties and transmutations of chemical elements important for processes powering the *engines* which drive many sites of the Universe: life on the Earth, an evolution of stars, galaxies, etc. These are the fusion reactions of light nuclides that give the predominant energy source in the stars. Iron gives the final ash for nuclear reaction sequences at hydrostatic burning. The thermonuclear fusion reactors are the respective counterpart at the Earth based environment. Magnetically confined fusion plasma, or the Tokamak reactors are viewed as promising direction and respective future experimental facility ITER aims to make a bridge from plasma physics to future electricity-producing fusion power plants.

Nova and supernova represent plausible astrophysical site candidates for synthesis of heavy atomic nuclei and renewing other nuclear components. Magnetization of hot dense astrophysical plasma in vicinity of the neutrino sphere is crucial for occurrence an explosion and can leave its trace in nucleosynthesis. Such spectacular astronomical phenomena yield, in particular, the actinides containing basic fuel for nuclear fission reactors, among others. As we have seen, the efforts towards a better understanding of astrophysical nuclear transmutation problems are important not only for fundamental research, but capable to explore new ideas for nuclear fuel cycle technology. For instance, the problems of high-level toxic radioactive waste might be overcome by, e.g., construction and operation the Transmutation Facilities (e.g., Accelerator-Driven System — ADS) including the nuclear reaction networks similar to those occurred at nucleosynthesis in astrophysical plasmas. Therefore, the joint efforts in nuclear astrophysics and nuclear technology would be highly beneficial for both sides, and can provide an opportunity for a contribution to the solution of problems surrounding decommissioning and utilization of spent fuel and the nuclear powerplants themselves, especially, annealing the radioactive toxic nuclear waste.

This work is supported in part by the JINR, Dubna, Russia and the VIRGO observatory at the Physical Faculty, Taras Shevchenko National University of Kiev, Ukraine.

REFERENCES

1. *Bohr A., Mottelson B. R.* Nuclear Structure. N.Y.: Benjamin, 1969.
2. *Moiseenko S. G., Bisnovatyj-Kogan G. S., Ardeljan N. V.* A Magnetorotational Core-Collapse Model with Jets // MNRAS. 2006. V. 370. P. 501
3. *Kondratyev V. N.* Statistics of Magnetic Noise in Neutron Star Crusts // Phys. Rev. Lett. 2002. V. 88. P. 221101.

4. *Kondratyev V. N.* Neutron Capture Reactions in Strong Magnetic Fields of Magnetars // Phys. Rev. C. 2004. V. 69. P. 038801.
5. *Kondratyev V. N., Kadenko I. M.* Nucleosynthesis in Strong Magnetic Fields at Statistical Equilibrium // MNRAS. 2005. V. 359. P. 927
6. *Möller P., Nix J. R., Myers W. D., Swiatecki W. J.* Nuclear Ground State Masses and Deformations // At. Data Nucl. Data Tables. 1995. V. 59. P. 185

Received on October 23, 2007.

Корректор *Т. Е. Попеко*

Подписано в печать 20.03.2008.

Формат 60 × 90/16. Бумага офсетная. Печать офсетная.

Усл. печ. л. 1,43. Уч.-изд. л. 2,02. Тираж 350 экз. Заказ № 56128.

Издательский отдел Объединенного института ядерных исследований
141980, г. Дубна, Московская обл., ул. Жолио-Кюри, 6.

E-mail: publish@jinr.ru

www.jinr.ru/publish/